Inorg. Chem. **2002**, *41*, 3859–3865

Reaction of Bis(phosphine)(hydrotris(3,5-dimethylpyrazolyl)borato)rhodium(I) with Phenylacetylene, *p*-Nitrobenzaldehyde, and Triphenyltin Hydride: Structures of $[Rh(Tp^*)(PPh_3)_2]$, $[Rh(Tp^*)(H)(C_2Ph)\{P(4\text{-}C_6H_4F)_3\}]$, $[Rh(Tp^*)(H)(COC_6H_4\text{-}4\text{-}NO_2)(PPh_3)]$, and $[Rh(Tp^*)(H)(SnPh_3)(PPh_3)]$

Viorel Cîrcu, Manuel A. Fernandes, and Laurence Carlton*

Molecular Sciences Institute, School of Chemistry, University of the Witwatersrand, Johannesburg, Republic of South Africa

Received November 26, 2001

The complexes $[Rh(Tp^*)(PPh_3)_2]$ (**1a**) and $[Rh(Tp^*)\{P(4\text{-}C_6H_4F)_3\}_2]$ (**1b**) combine with PhC_2H, $4\text{-}NO_2\text{-}C_6H_4CHO$ and Ph_3SnH to give $[Rh(Tp^*)(H)(C_2Ph)(PR_3)]$ (R = Ph, **2a**; R = $4\text{-}C_6H_4F$, **2b**), $[Rh(Tp^*)(H)(COC_6H_4\text{-}4\text{-}NO_2)(PR_3)]$ (R = Ph, **3a**), and $[Rh(Tp^*)(H)(SnPh_3)(PR_3)]$ (R = Ph, **4a**; R = $4\text{-}C_6H_4F$, **4b**) in moderate to good yield. Complexes **1a**, **2b**, **3a,** and **4a** have been structurally characterized. In **1a** the Tp* ligand is bidentate, in **2b**, **3a**, and **4a** it is tridentate. Crystal data for **1a**: space group $P2_1/c$; a = 11.9664(19), b = 21.355(3), c = 20.685(3) Å; β = 112.576(7)°; V = 4880.8(12) Å^3; Z = 4; R = 0.0441. Data for **2b**: space group $P\bar{1}$; a = 10.130(3), b = 12.869(4), c = 17.038(5) Å; α = 78.641(6), β = 76.040(5), γ = 81.210(6)°; V = 2100.3(11) Å^3; Z = 2; R = 0.0493. Data for **3a**: space group $P\bar{1}$; a = 10.0073(11), b = 10.5116(12), c = 19.874(2) Å; α = 83.728(2), β = 88.759(2), γ = 65.756(2)°; V =1894.2(4) Å^3; Z = 2; R = 0.0253. Data for **4a**: space group $P2_1/c$; a = 15.545(2), b = 18.110(2), c = 17.810(2) Å; β = 95.094(3)°; V = 4994.1(10) Å^3; Z = 4; R = 0.0256. NMR data (^{1}H, ^{31}P, ^{103}Rh, ^{119}Sn) are also reported.

Introduction

The complex $[Rh(Tp)(PPh_3)_2]$ (Tp = hydrotris(pyrazolyl)-borate), recently reported by Hill and co-workers,[1] provides a useful route to a variety of Rh(Tp) derivatives. The potential of the Tp ligand to modify the properties of metals (notably rhodium and iridium) in ways related to the activation of C−H and other bonds was first recognized by Ghosh and Graham,[2] and much subsequent work with Tp complexes has sought to expand on this knowledge.[3] In this connection we report the preparation of $[Rh(Tp^*)(PPh_3)_2]$ and $[Rh(Tp^*)\{P(4\text{-}C_6H_4F)_3\}_2]$ (Tp* = hydrotris(3,5-dimethylpyrazolyl)borate) and their reaction with PhC_2H, $4\text{-}NO_2C_6H_4CHO$, and Ph_3SnH.

Experimental Section

Materials. $[Rh(Cl)(PPh_3)_3]$ and $[Rh(Cl)\{P(4\text{-}C_6H_4F)_3\}_3]$ were prepared according to the method of Wilkinson.[4] KTp* and Ph_3SnH were purchased from Aldrich Chemicals. Dichloromethane was distilled from P_2O_5. Other solvents and materials were of the highest available purity and were used without further treatment. All operations were performed under a nitrogen atmosphere.

Preparation of $[Rh(Tp^*)(PPh_3)_2](EtOH)$ (1a). A slightly modified version of the method of Hill et al.[1] was used. A suspension of $[Rh(Cl)(PPh_3)_3]$ (1.000 g, 1.081 mmol) and KTp*

* To whom correspondence should be addressed. E-mail: carlton@aurum.chem.wits.ac.za. Fax: +27 11 717 6749.

(1) Hill, A. F.; White, A. J. P.; Williams, D. J.; Wilton-Ely, J. D. E. T. *Organometallics* **1998**, *17*, 3152.
(2) Ghosh, C. K.; Graham, W. A. G. *J. Am. Chem. Soc*. **1987**, *109*, 4726.
(3) (a) Ghosh, C. K.; Graham, W. A. G. *J. Am. Chem. Soc.* **1989**, *111*, 375. (b) Bloyce, P. E.; Mascetti, J.; Rest, A. J. *J. Organomet. Chem.* **1993**, *444*, 223. (c) Purwoko, A. A.; Lees, A. J. *Inorg. Chem*. **1995**, *34*, 424. (d) Paneque, M.; Taboada, S.; Carmona, E. *Organometallics* **1996**, *15*, 2678. (e) Wick, D. D.; Northcutt, T. O.; Lachicotte, R. J.; Jones, W. D. *Organometallics* **1998**, *17*, 4484. (f) Paneque, M.; Poveda, M. L.; Salazar, V.; Taboada, S.; Carmona, E. *Organometallics* **1999**, *18*, 139. (g) Gutiérrez-Puebla, E.; Monge, A.; Paneque, M.; Poveda, M. L.; Salazar, V.; Carmona, E. *J. Am. Chem. Soc*. **1999**, *121*, 248. (h) Wick, D. D.; Jones, W. D. *Organometallics* **1999**, *18*, 495. (i) Paneque, M.; Pérez, P. J.; Pizzano, A.; Poveda, M. L.; Taboada, S.; Trujillo, M.; Carmona, E. *Organometallics* **1999**, *18*, 4304. (j) Wick, D. D.; Reynolds, K. A.; Jones, W. D. *J. Am. Chem. Soc*. **1999**, *121*, 3974. (k) Tellers, D. M.; Bergman, R. G. *J. Am. Chem. Soc*. **2000**, *122*, 954. (l) Wiley, J. S.; Oldham, W. J.; Heinekey, D. M. *Organometallics* **2000**, *19*, 1670. (m) Yeston, J. S.; Bergman, R. G. *Organometallics* **2000**, *19*, 2947. (n) Slugovc, C.; Padilla-Martinez, I.; Sirol, S.; Carmona, E. *Coord. Chem. Rev.* **2001**, *213*, 129.
(4) Osborn, J. A.; Wilkinson, G. *Inorg. Synth*. **1967**, *10*, 67.

10.1021/ic0112037 CCC: $22.00
Published on Web 06/28/2002

(0.375 g, 1.115 mmol) in EtOH (25 mL) was heated under reflux for 30 min, during which time the color changed from red-purple to yellow. A yellow powder was collected by filtration of the hot mixture, washed with EtOH and a small quantity of diethyl ether, and recrystallized from ~2:1 CH_2Cl_2/EtOH. The product was obtained as orange crystals. Yield: 0.690 g (66%). IR (KBr): ν(BH) 2457 (m) cm^{-1}. ^1H NMR ($CDCl_3$, 213 K): δ 7.0 (s (br), 30H, PC_6H_5), 5.84 (s, 2H, pz* H^4) 5.37 (s, 1H, pz* H^4) 4.45 (s (br), 1H, BH), 2.56 (s, 3H, pz* Me) 2.29 (s, 6H, pz* Me) 2.26 (s, 3H, pz* Me) 1.77 (s(br), 6H, pz* Me). Anal. Calcd for $C_{53}H_{58}BN_6OP_2Rh$: C, 65.58; H, 6.02; N, 8.66. Found C, 65.05; H, 5.77; N, 8.72.

Preparation of [Rh(Tp*){P(4-C_6H_4F)$_3$}$_2$](EtOH) (1b). A suspension of [Rh(Cl){P(4-C_6H_4F)$_3$}$_2$] (0.500 g, 0.460 mmol) and KTp* (0.200 g, 0.595 mmol) in ethanol (10 mL) was heated under reflux for 30 min, during which time the color changed to yellow. A yellow powder was collected by filtration of the hot mixture, washed with ethanol, and recrystallized from ~2:1 dichloromethane/ethanol. The product was obtained as yellow-orange crystals. Yield: 0.315 g (64%). IR (KBr): ν(BH) 2473 (m) cm^{-1}. ^1H NMR ($CDCl_3$, 213 K): δ 6.7. (s (br), 24H PC_6H_4F), 5.88 (s, 2H, pz* H^4), 5.37 (s, 1H, pz* H^4), 4.41 (s (br), 1H, BH), 2.52 (s, 3H, pz* Me), 2.28 (s, 6H, pz* Me), 2.34 (s, 3H, pz* Me), 1.71 (s (br) 6H, pz* Me). Anal. Calcd for $C_{53}H_{52}BF_6N_6OP_2Rh$: C, 59.01; H, 4.86; N, 7.79. Found: C, 59.11; H, 4.78; N, 7.90.

Preparation of [Rh(Tp*)(H)(C_2Ph)(PPh$_3$)] (2a). A solution of **1a** (0.050 g, 0.051 mmol) in dichloromethane (2 mL) at room temperature was treated with phenylacetylene (0.02 g, 0.20 mmol) and allowed to stand for 1 h. A color change from orange to yellow was observed. On concentration of the solution and addition of ethanol, colorless crystals were obtained which were recrystallized from dichloromethane/ethanol. Yield: 0.033 g (85%). IR (KBr): ν(BH) 2518 (m), ν(CC) 2111 (s) cm^{-1}. ^1H NMR ($CDCl_3$, 300 K): δ 7.6−7.0 (mults, 20H, C_6H_5, PC_6H_5), 5.66, 5.65, 5.11 (s × 3, 3H, pz* H^4), 5.0−4.1 (br, 1H, BH; s (br) 4.55 ppm at 213 K), 2.74, 2.47, 2.29, 2.21, 1.42, 1.39 (s × 6, 18H, pz* Me), −14.82 (dd (J = 22.2, 16.6), 1H, RhH). Anal. Calcd for $C_{41}H_{43}BN_6PRh$: C, 64.41; H, 5.67; N, 10.99. Found: C, 64.44; H, 5.73; N, 10.85.

Preparation of [Rh(Tp*)(H)(C_2Ph){P(4-C_6H_4F)$_3$}] (2b). A solution of **1b** (0.050 g, 0.046 mmol) in dichloromethane (2 mL) at room temperature was treated with phenylacetylene (0.02 g, 0.20 mmol) and allowed to stand for 1 h. The solution was concentrated and treated with ethanol to give a white powder which was recrystallized from dichloromethane/ethanol to give colorless microcrystalline needles (which were used to obtain CHN data; slow crystallization gave crystals suitable for X-ray work). Yield: 0.030 g (80%). IR (KBr): ν(BH) 2523 (m), ν(CC) 2111 (s) cm^{-1}. ^1H NMR ($CDCl_3$, 300 K): δ 7.6−6.6 (mults, 17H, C_6H_5, PC_6H_4F), 5.68, 5.65, 5.20 (s × 3, 3H, pz* H^4), 5.1−4.1 (br, 1H, BH; s (br), 4.54 ppm at 213 K), 2.71, 2.47, 2.31, 2.21, 1.48, 1.38 (s × 6, 18H, pz* Me), −14.88 (dd (J = 22.5, 16.7), 1H, RhH). Anal. Calcd for $C_{41}H_{40}BF_3N_6PRh$: C, 60.16; H, 4.93; N, 10.27. Found: C, 60.30; H, 5.05; N, 10.17.

Preparation of [Rh(Tp*)(H)(COC$_6$H$_4$-4-NO$_2$)(PPh$_3$)] (3a). A mixture of **1a** (0.050 g, 0.051 mmol) and 4-$NO_2C_6H_4CHO$ (0.020 g, 0.132 mmol) dissolved in benzene (2 mL) was heated for 90 min at 70 °C. A color change from orange to red was observed. The solution was allowed to cool before treating with hexane (3 mL) and centrifuged to remove a small quantity of a flocculent material. On standing at room temperature for 3 d, amber crystals were obtained. Yield: 13 mg (31%). IR (KBr): ν(BH) 2524 (m), ν(RhH) 2078 (m). ^1H NMR ($CDCl_3$, 300 K): δ 7.71 (d, 2H (J = 8.9), $C_6H_4NO_2$), 7.5−7.0 (mults (br), 15H, PC_6H_5), 7.06 (d, 2H (J = 8.9), $C_6H_4NO_2$), 5.68, 5.55, 5.09 (s × 3, 3H, pz* H^4), 5.2−4.3 (br, 1H, BH; s (br), 4.72 ppm at 213 K), 2.62, 2.37, 2.30, 1.82, 1.40, 0.40 (s × 6, 18H, pz* Me), −13.81 (dd (J = 18.9, 13.1), 1H, RhH). Anal. Calcd for $C_{40}H_{42}BN_7O_3RhP$: C, 59.06; H, 5.20; N, 12.05. Found: C, 59.28; H, 5.52; N, 11.56.

Preparation of [Rh(Tp*)(H)(SnPh$_3$)(PPh$_3$)](CH$_2$Cl$_2$) (4a). A solution of **1a** (0.050 g, 0.052 mmol) in dichloromethane (2 mL) at room temperature was treated with triphenyltin hydride (0.030 g, 0.085 mmol) and allowed to stand for 30 min, during which time a color change from orange to yellow was observed. The solution was concentrated and ethanol was added to give yellow crystals which were recrystallized from dichloromethane/ethanol. Yield: 0.035 g (63%). IR (KBr): ν(BH) 2519 (m), ν(RhH) 2072 (m) cm^{-1}. ^1H NMR ($CDCl_3$, 300 K): δ 7.3−6.8 (mults, 30H, PC_6H_5, SnC_6H_5), 5.70, 5.26, 5.17 (s × 3, 3H, pz* H^4), 5.2−4.3 (br, 1H, BH; s (br), 4.73 ppm at 213 K), 2.68, 2.41, 2.26, 1.74, 1.61, 0.87 (s × 6, 18H, pz* Me), −15.19 (dd (J = 22.0, 10.1), 1H, RhH). Anal. Calcd for $C_{52}H_{55}BCl_2N_6PRhSn$: C, 56.86; H, 5.05; N, 7.65. Found: C, 56.87; H, 5.14; N, 7.61.

Preparation of [Rh(Tp*)(H)(SnPh$_3$){P(4-C_6H_4F)$_3$}] (4b). A solution of **1b** (0.050 g, 0.046 mmol) in dichloromethane (2 mL) at room temperature was treated with triphenyltin hydride (0.030 g, 0.085 mmol) and allowed to stand for 1 h. The solution was concentrated, and ethanol was added to give a yellow oil, which was crystallized twice from dichloromethane/ethanol. The product was obtained as yellow crystals. Yield: 0.027 g (55%). IR (KBr): ν(BH) 2524 (m), ν(RhH) 2094 (m) cm^{-1}. ^1H NMR ($CDCl_3$, 300 K): δ 7.3−6.5 (mults, 27H, PC_6H_4F, SnC_6H_5), 5.73, 5.29, 5.26 (s × 3, 3H, pz* H^4), 5.3−4.3 (br, 1H, BH; s (br), 4.72 ppm at 213 K), 2.68, 2.42, 2.26, 1.73, 1.61, 0.95 (s × 6, 18H, pz* Me), −15.20 (dd (J = 22.3, 10.2), 1H, RhH). Anal. Calcd for $C_{51}H_{50}BF_3N_6PRhSn$: C, 57.39; H, 4.72; N, 7.87. Found: C, 57.15; H, 4.74; N, 7.52.

NMR Spectroscopy. Spectra were recorded on a Bruker DRX 400 spectrometer equipped with a 5 mm triple resonance inverse probe with a dedicated ^{31}P channel and extended decoupler range operating at 400.13 MHz (^1H), 161.98 MHz (^{31}P), 12.65 MHz (^{103}Rh), and 149.21 MHz (^{119}Sn). Two-dimensional $^{103}Rh-^{31}P$ spectra were obtained using the pulse sequence $\pi/2(^{31}P)-1/[2J(^{103}Rh-^{31}P)]-\pi/2(^{103}Rh)-\tau-\pi(^{31}P)-\tau-\pi/2(^{103}Rh)-1/[2J(^{103}Rh-^{31}P)]-Acq(^{31}P)$.[5] Further details are given in ref 6. Chemical shifts were referenced to the generally accepted standards of 85% H_3PO_4, $\Xi(^{103}Rh)$ = 3.16 MHz,[7] and $SnMe_4$, with positive values indicating deshielding. The chemical shifts of H_3PO_4 (with CD_2Cl_2 external lock, 300 K) and $SnMe_4$ (CD_2Cl_2 external lock 248 K) correspond to frequencies of 161.975 500 and 149.210 995 MHz, respectively, in a field (9.395 T) in which the protons of TMS (in CD_2Cl_2 at 300 K) resonate at 400.130 020 MHz.

X-ray Structure Determination. Intensity data were collected at 20 °C (**1a**) and −100 °C (**2b**, **3a**, **4a**) on a Bruker SMART 1K CCD area detector diffractometer with graphite-monochromated Mo Kα radiation (50 kV, 30 mA). The collection method involved ω-scans of width 0.3°. Data reduction was carried out using the program SAINT+,[8] and absorption corrections were made using the program SADABS.[9] The crystal structures were solved by direct

(5) Bax, A.; Griffey, R. H.; Hawkins, B. L. *J. Magn. Reson.* **1983**, *55*, 301.
(6) Carlton, L. *Inorg. Chem.* **2000**, *39*, 4510.
(7) Kidd, R. G.; Goodfellow, R. J. In *NMR and the Periodic Table*; Harris, R. K., Mann, B. E., Eds.; Academic Press: London, 1978; pp 244−249.
(8) *SAINT+*, version 6.02; Bruker AXS Inc.: Madison, WI, 1999.
(9) Sheldrick, G. M. *SADABS*; University of Göttingen: Göttingen. Germany, 1996.

Table 1. Crystal Data and Structure Refinement for **1a**, **2b**, **3a**, and **4a**

	[Rh(Tp*)(PPh$_3$)$_2$]-(EtOH) (**1a**)	[Rh(Tp*)(H)(C$_2$Ph)-{P(C$_6$H$_4$F)$_3$}](CH$_2$Cl$_2$) (**2b**)	[Rh(Tp*)(H)-(COC$_6$H$_4$NO$_2$)(PPh$_3$)] (**3a**)	[Rh(Tp*)(H)(SnPh$_3$)-(PPh$_3$)](CH$_2$Cl$_2$) (**4a**)
empirical formula	$C_{53}H_{58}BN_6OP_2Rh$	$C_{42}H_{42}BCl_2F_3N_6PRh$	$C_{40}H_{42}BN_7O_3PRh$	$C_{52}H_{55}BCl_2N_6PRhSn$
fw	970.71	903.41	813.50	1098.30
temp (K)	293(2)	173(2)	173(2)	173(2)
wavelength (Å)	0.71073	0.71073	0.71073	0.71073
cryst system	monoclinic	triclinic	triclinic	monoclinic
space group	$P2_1/c$	$P\bar{1}$	$P\bar{1}$	$P2_1/c$
unit cell dimens	a = 11.9664(19) Å	a = 10.130(3) Å	a = 10.0073(11) Å	a = 15.545 (2) Å
	b = 21.355(3) Å	b = 12.869(4) Å	b = 10.5116(12) Å	b = 18.110(2) Å
	c = 20.685(3) Å	c = 17.038(5) Å	c = 19.874(2) Å	c = 17.810(2) Å
	α = 90°	α = 78.641(6)°	α = 83.728(2)°	α = 90°
	β = 112.576(7)°	β = 76.040(5)°	β = 88.759(2)°	β = 95.094(3)°
	γ = 90°	γ = 81.210(6)°	γ = 65.756(2)°	γ = 90°
V (Å^3)	4880.8(12)	2100.3(11)	1894.2(4)	4994.1(10)
Z	4	2	2	4
density (calcd) (Mg/m^3)	1.321	1.428	1.426	1.461
abs coeff (mm^{-1})	0.460	0.623	0.541	1.011
F(000)	2024	924	840	2232
cryst size (mm^3)	0.35 × 0.24 × 0.09	0.44 × 0.14 × 0.12	0.49 × 0.38 × 0.16	0.38 × 0.20 × 0.14
θ range for data collcn (deg)	1.43−28.31	1.25−26.00	2.06−28.29	1.32−28.31
index ranges	$-15 \le h \le 15$	$-12 \le h \le 12$	$-12 \le h \le 13$	$-18 \le h \le 20$
	$-28 \le k \le 28$	$-15 \le k \le 9$	$-7 \le k \le 13$	$-21 \le k \le 24$
	$-27 \le l \le 23$	$-19 \le l \le 21$	$-25 \le l \le 26$	$-23 \le l \le 13$
reflcns collcd	33868	11821	13183	34289
indepdt reflcns	12032 [R(int) = 0.0446]	8116 [R(int) = 0.0276]	9088 [R(int) = 0.0112]	12202 [R(int) = 0.0222
completeness to θ_{max} (%)	99.1	98.2	96.5	98.3
max and min transm	0.9598 and 0.8556	0.9290 and 0.7711	0.9184 and 0.7773	0.8714 and 0.6999
data/restraints/params	12032/1/577	8116/1/513	9088/0/489	12202/0/591
goodness-of- fit on F^2	0.988	1.028	1.039	1.034
final R indices [$I > 2\sigma(I)$]	R1 = 0.0441	R1 = 0.0493	R1 = 0.0253	R1 = 0.0256
	wR2 = 0.1093	wR2 = 0.1228	wR2 = 0.0628	wR2 = 0.0609
R indices (all data)	R1 = 0.0880	R1 = 0.0714	R1 = 0.0304	R1 = 0.0364
	wR2 = 0.1237	wR2 = 0.1363	wR2 = 0.0651	wR2 = 0.0648
largest diff peaks (e Å^{-3})	1.319 and −0.539	1.772 and −1.601	0.462 and −0.339	1.177 and −1.168

methods using SHELXTL.[10] Non-hydrogen atoms were first refined isotropically followed by anistropic refinement by full-matrix least-squares calculation based on F^2 using SHELXTL. With the exception of H(2) in **3a** and **4a** all hydrogen atoms were placed geometrically and allowed to ride on their respective parent atoms. The hydride ligand H(2) in **3a** and **4a** was placed by means of the difference map and refined isotropically. X-ray data are found in Table 1. Diagrams were generated using SHELXTL and PLATON.[11]

Results and Discussion

The complexes [Rh(Tp*)(PPh$_3$)$_2$] (**1a**) and [Rh(Tp*){P(4-C$_6$H$_4$F)$_3$}$_2$] (**1b**) are easily prepared and are potentially valuable precursors to a variety of compounds containing the Rh(Tp*) fragment. This has been noted by Hill,[1] with respect to the related complex [Rh(Tp)(PPh$_3$)$_2$], in addition to possible catalytic activity. The air sensitivity of **1a** in solution is rather low, oxidation (to unidentified products) occurring over a period of hours. Compounds having weakly acidic hydrogen atoms react readily with **1a,b**, although in some cases products are obtained in which only a fragment of the Tp* ligand remains.[12] With PhC$_2$H, 4-NO$_2$C$_6$H$_4$CHO, and Ph$_3$SnH oxidative addition products **2**−**4** are formed in moderate to good yield (Scheme 1).

Structures. In the complex [Rh(Tp*)(PPh$_3$)$_2$] (**1a**, Figure 1) the Tp* ligand is bound in a bidentate manner, giving a slightly distorted square planar geometry at the metal with the angle N(22)−Rh−N(32) significantly smaller than 90° and P(1)−Rh−P(2) significantly larger (see Table 2). Steric repulsion between the two phosphines is likely to be the major contributor to this effect: the distortions found in the related square planar complexes [Rh(Tp*)(CO)(PPh$_3$)][13] and [Rh(Tp^{Ph,Me})(CO)(PPh$_3$)][14] are much smaller, while the Rh−N and Rh−P bond lengths do not differ greatly from those of **1a**. A phenyl hydrogen (H(96)) occupies a position directly above one of the vacant coordination sites at a distance of 3.06(2) Å from the metal. An interaction of this

Scheme 1

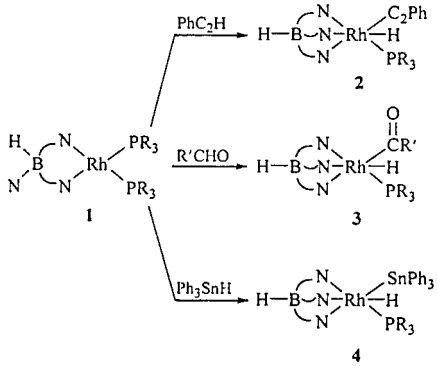

(10) *SHELXTL*, version 5.1; Bruker AXS Inc.: Madison, WI, 1999.
(11) Spek, A. L. *Acta Crystallogr.* **1990**, *A46*, C34.
(12) Cîrcu, V.; Fernandes, M. A.; Carlton, L. Paper in preparation.
(13) Connelly, N. G.; Emslie, D. J. H.; Metz, B.; Orpen, A. G.; Quayle, M. J. *J. Chem. Soc., Chem. Commun.* **1996**, 2289.
(14) Moszner, M.; Wolowiec, S.; Trösch, A.; Vahrenkamp, H. *J. Organomet. Chem.* **2000**, *595*, 178.

Table 2. Selected Bond Lengths (Å) and Angles (deg) for **1a**, **2b**, **3a**, and **4a**

	[Rh(Tp*)(PPh$_3$)$_2$](EtOH) (**1a**)	Rh(Tp*)(H)(C$_2$Ph)-{P(C$_6$H$_4$F)$_3$}](CH$_2$Cl$_2$) (**2b**)	[Rh(Tp*)(H)-(COC$_6$H$_4$NO$_2$)(PPh$_3$)] (**3a**)	[Rh(Tp*)(H)(SnPh$_3$)-(PPh$_3$)](CH$_2$Cl$_2$) (**4a**)
Rh−N(12)		2.250(3)	2.2139(14)	2.2099(16)
Rh−N(22)	2.140(2)	2.104(3)	2.1085(14)	2.1468(16)
Rh−N(32)	2.086(2)	2.113(3)	2.2031(14)	2.1864(17)
Rh−H(2)		1.4406	1.49(2)	1.42(2)
Rh−P(1)	2.2669(9)	2.2751(11)	2.2925(4)	2.2906(5)
Rh−X[a]	2.2803(8)	1.973(4)	1.9933(17)	2.5991(3)
C(72)−O(71)			1.228(2)	
C(71)−C(72)		1.207(6)		
N(12)−Rh−N(22)		83.85(12)	86.19(5)	84.54(6)
N(12)−Rh−N(32)		92.19(12)	92.12(5)	94.16(6)
N(22)−Rh−N(32)	78.13(9)	81.86(12)	80.08(5)	79.29(6)
N(12)−Rh−H(2)		180.0	176.4(8)	174.9(9)
N(22)−Rh−H(2)		96.2	90.2(8)	91.9(9)
N(32)−Rh−H(2)		87.8	87.7(8)	88.7(9)
N(12)−Rh−P(1)		99.70(8)	96.99(4)	93.37(4)
N(22)−Rh−P(1)	166.84(7)	176.24(9)	173.00(4)	171.58(5)
N(32)−Rh−P(1)	91.33(7)	96.69(9)	93.54(4)	92.76(5)
N(12)−Rh−X[a]		94.03(13)	95.04(6)	99.24(4)
N(22)−Rh−X[a]	94.28(7)	95.02(14)	95.26(6)	91.46(5)
N(32)−Rh−X[a]	168.79(7)	172.71(14)	171.19(6)	162.94(4)
P(1)−Rh−X[a]	97.23(3)	86.01(12)	90.68(5)	96.929(16)
P(1)−Rh− H(2)		80.3	86.6(8)	90.7(9)
H(2)−Rh−X[a]		86.0	84.8(8)	77.2(9)
Rh−C(71)−C(72)		176.1(3)		
Rh−C(72)−C(73)			121.98(11)	
Rh−C(72)−O(71)			123.88(12)	

[a] X = phosphorus P(2) (**1a**), carbon C(71) (**2b**), carbon C(72) (**3a**), and tin (**4a**).

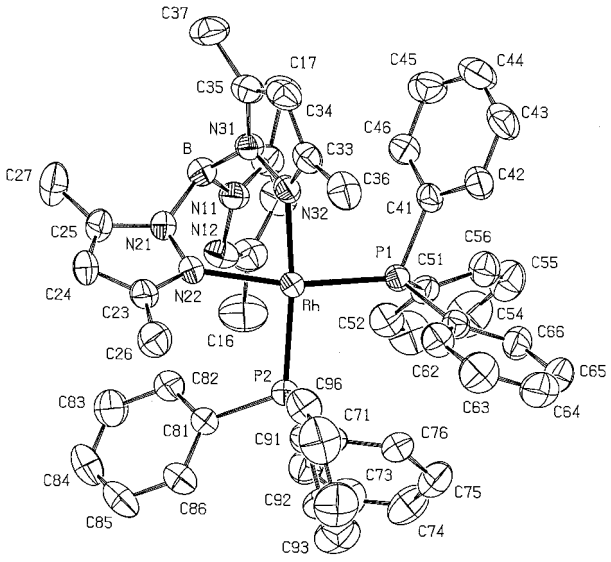

Figure 1. ORTEP diagram of [Rh(Tp*)(PPh$_3$)$_2$] (**1a**). Thermal ellipsoids are shown at the 50% probability level. Hydrogens and a cocrystallized EtOH are omitted.

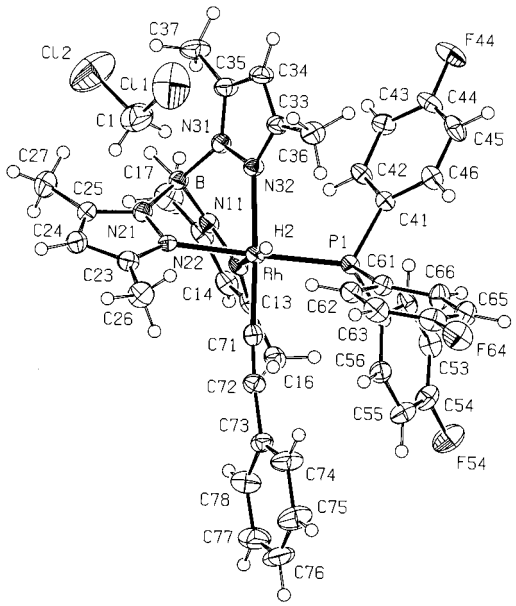

Figure 2. ORTEP diagram of [Rh(Tp*)(H)(C$_2$Ph){P(4-C$_6$H$_4$F)$_3$}](CH$_2$Cl$_2$) (**2b**). Thermal ellipsoids are shown at the 50% probability level. The position of the hydride ligand is calculated (the hydride was not located).

type is found in [Rh(Cl)(PPh$_3$)$_3$],[15] giving rise to the two allotropic forms (the Rh···H distance in the red form of [Rh(Cl)(PPh$_3$)$_3$] is 2.77 Å, and that in the orange form, 2.84 Å).

Complexes **2**−**4** are chiral. Both enantiomers are present in these structures and are related to each other by an inversion center. The acetylide complex **2b** (Figure 2) has Rh−C and C≡C bond distances and Rh−C−C angle comparable to those reported for the complexes [Rh(C$_2$Ph)(PMe$_3$)$_4$],[16] [Rh(C$_2$Ph)$_2$(H)(PMe$_3$)$_4$],[17] [Rh(C$_4$H$_7$N$_2$O$_2$)$_2$(C$_2$Ph)(PPh$_3$)],[18] and [Rh(C$_2$Ph)$_2$(SnPh$_3$)(PMe$_3$)$_3$].[19] Similarly the Rh−C and CO bond distances and Rh−C−O and Rh−C−C angles of **3a** (Figure 3) resemble those of [Rh(Ph$_2$P(CH$_2$)$_3$PPh$_2$)(Cl)$_2$(COPh)],[20] [Rh(COPh)(Et$_4$Me$_4$porphinate)],[21] [RhCl$_2$-

(15) Bennett, M. J.; Donaldson, P. B. *Inorg. Chem.* **1977**, *16*, 655.
(16) Zargarian, D.; Chow, P.; Taylor, N. J.; Marder, T. B. *J. Chem. Soc., Chem. Commun.* **1989**, 540.
(17) Chow, P.; Zargarian, D.; Taylor, N. J.; Marder, T. B. *J. Chem. Soc., Chem. Commun.* **1989**, 1545.
(18) Dunaj-Jurčo, M.; Kettmann, V.; Steinborn, D.; Ludwig, M. *Acta Crystallogr*. **1995**, *C51*, 210.
(19) Werner, H.; Gevert, O.; Haquette, P. *Organometallics* **1997**, *16*, 803.
(20) McGuiggan, M. F.: Doughty, D. H.; Pignolet, L. H. *J. Organomet. Chem*. **1980**, *185*, 241.

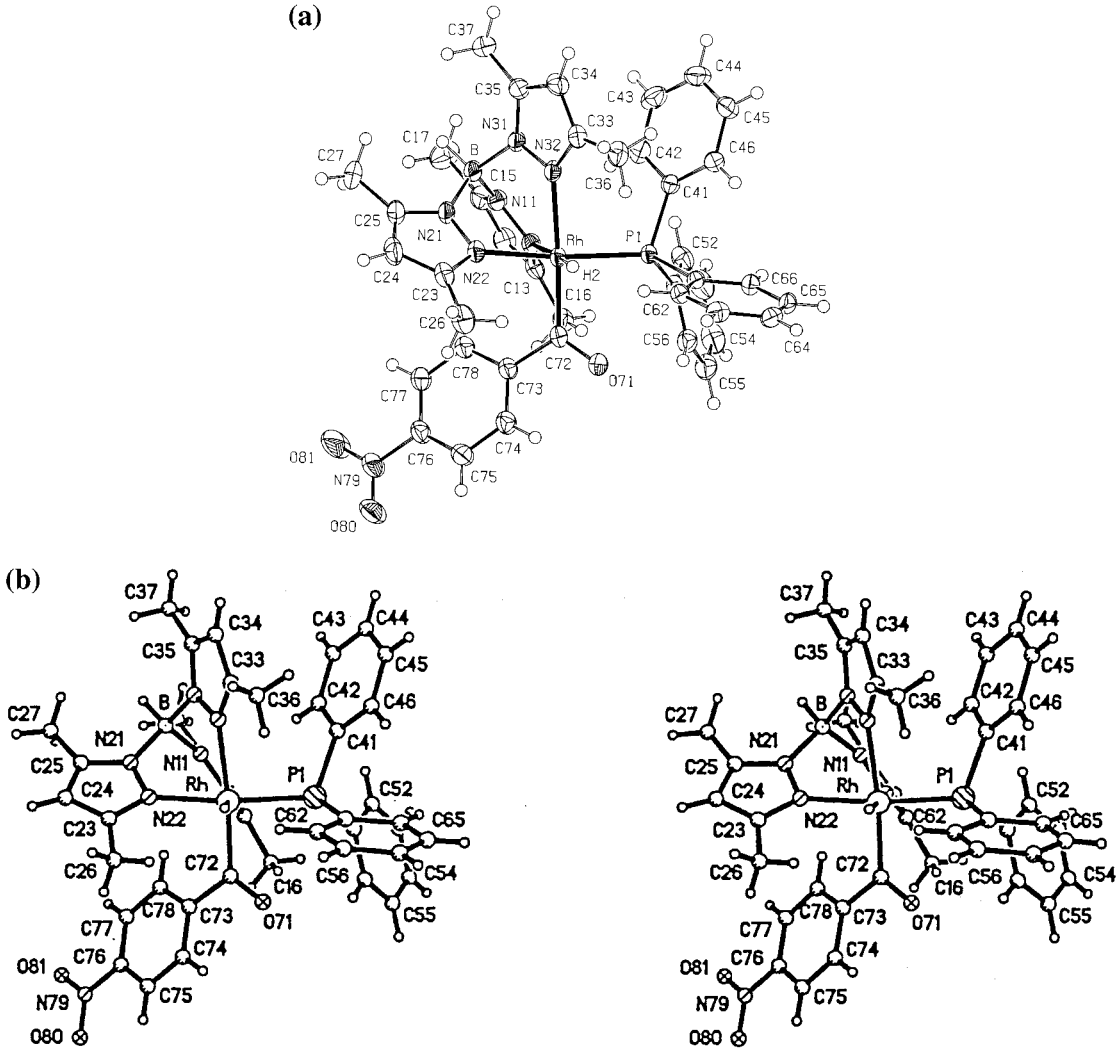

Figure 3. (a) ORTEP diagram of [Rh(Tp*)(H)(COC$_6$H$_4$-4-NO$_2$)(PPh$_3$)] (**3a**). Thermal ellipsoids are shown at the 50% probability level. The hydride ligand was located. (b) Stereoview of **3a**.

(COCH$_3$){2,6(CHN^{t}Bu)$_2$C$_6$H$_3$N}],[22] [Rh{N(CH$_2$CH$_2$PPh$_2$)$_3$}-(H)(COMe)]BPh$_4$,[23a] and [Rh(COPh)(H)(Cl)(P^{i}Pr$_3$)$_2$].[24] In the last of these compounds a C−Rh−H angle of 85° is found, identical, within error limits, to that of **3a**. This angle is small for atoms in the equatorial plane of a trigonal bipyramidal structure and is attributed by the authors to a close contact (1.85 Å) between the hydride ligand and an ortho hydrogen of the benzoyl group. No such contact is found between the hydride of **3a** and the *p*-nitrobenzoyl hydrogens, but a fairly close contact is found between the hydride and an ortho hydrogen of a phenyl group of triphenylphosphine (H(2)−H(62) = 2.08(2) Å). A similar geometry is found for both **2b** and **4a**.

The Rh−Sn (2.599 Å) bond of the triphenyltin complex **4a** (Figure 4) lies midway between the distances reported for [Rh(C$_2$Ph)$_2$(SnPh$_3$)(PMe$_3$)$_3$][19] (2.640 Å) and [Rh(NCBPh$_3$)-(H)(SnPh$_3$)(PPh$_3$)$_2$][25] (2.559 Å). The Sn−H distance of 2.67-(2) Å indicates a weak interaction between tin and hydrogen.

NMR Spectroscopy. The solvation of complexes **1a,b** and **4a** was confirmed by their ^{1}H spectra. Data are presented in Table 3. The ^{1}H spectra of **1a,b** show broadening of the pyrazole CH and two (**1a**) or all (**1b**) of the CH$_3$ signals at 27 °C. The BH signal from all complexes (**1**−**4**) at this temperature is broadened to the point where it is not readily detected but becomes more clearly visible at −60 °C, at which temperature the pyrazole CH signals from **1a,b** become sharper and the signals from the phenyl protons become broadened. The ^{31}P{^{1}H} signal (doublet) from each (**1a,b**) is well resolved at 27 °C but broadened at −60 °C. These findings are consistent with a process involving interconversion between the favored four-coordinate η^2-Tp* and a five-coordinate η^3-Tp* coordination geometry. Addi-

(21) Grigg, R.; Trocha-Grimshaw, J.; Henrik, K. *Acta Crystallogr*. **1982**, *B38*, 2455.
(22) Haarman, H. F.; Kaagman, J.-W. F.; Smeets, W. J. J.; Spek, A. L.; Vrieze, K. *Inorg. Chim. Acta* **1998**, *270*, 34.
(23) (a) Bianchini, C.; Meli, A.; Peruzzini, M.; Vizza, F.; Bachechi, F. *Organometallics* **1991**, *10*, 820. (b) Bianchini, C.; Meli, A.; Peruzzini, M.; Ramirez, J. A.; Vacca, A.; Vizza, F.; Zanobini, F. *Organometallics* **1989**, *8*, 337.
(24) Wang, K.; Emge, T. J.; Goldman, A. S.; Li, C.; Nolan, S. P. *Organometallics* **1995**, *14*, 4929.
(25) Carlton, L.; Weber, R.; Levendis, D. C. *Inorg. Chem*. **1998**, *37*, 1264.

Table 3. NMR Spectral Data

complex[a]	$\delta(^1H)$[b]	$\delta(^{31}P)$[c]	$\delta(^{103}Rh)$[d]	$\delta(^{119}Sn)$[e]	$J(P-H)$[f]	$J(Rh-H)$[f]	$J(Sn-H)$[f,g]	$J(Rh-P)$[f]	$J(Sn-P)$[f,h]	$J(Rh-Sn)$[f]
$[Rh(Tp^*)(PPh_3)_2]$ (**1a**)[i]		42.16	329					175.7		
$[Rh(Tp^*)\{P(C_6H_4F)_3\}_2]$ (**1b**)		40.36	313					176.5		
$[Rh(Tp^*)(H)(C_2Ph)(PPh_3)]$ (**2a**)	−14.85	45.92	1423		21.9	16.8		131.2		
$[Rh(Tp^*)(H)(C_2Ph)\{P(C_6H_4F)_3\}]$ (**2b**)	−14.88	43.90	1417		22.2	16.8		131.9		
$[Rh(Tp^*)(H)(COC_6H_4NO_2)(PPh_3)]$ (**3a**)	−13.83	48.09	1730		13.1	18.9		163.3		
$[Rh(Tp^*)(H)(COC_6H_4NO_2)\{P(C_6H_4F)_3\}]$ (**3b**)[j]	−13.91	45.74	1727		12.8	19.3		164.6		
$[Rh(Tp^*)(H)(SnPh_3)(PPh_3)]$ (**4a**)[k]	−15.19	46.18	1302	−132.45	21.9	10.0	101.5	133.0	305	410
	(−14.95)[l]	(46.34)	(1236)	(−122.21)				(130.9)	(317)	(411)
$[Rh(Tp^*)(H)(SnPh_3)\{P(C_6H_4F)_3\}]$ (**4b**)[k]	−15.19	44.87	1283	−126.54	22.2	10.1	99.1	133.9	307	403
	(−14.96)[l]	(44.96)	(1220)	(−118.05)				(132.1)	(315)	(403)

[a] Solution (0.01−0.02 M) in CD_2Cl_2/CH_2Cl_2 at 300 K. [b] Chemical shift of RhH in ppm from TMS (internal standard). [c] Chemical shifts in ppm from 85% H_3PO_4 (external standard). [d] Chemical shifts in ppm from $\Xi = 3.16$ MHz. [e] Chemical shifts in ppm from $SnMe_4$ (external standard) at 248 K. Relative to $SnMe_4$ at 300 K signals lie 0.39 ppm to higher δ. [f] Coupling constants (absolute magnitude) in Hz. Signs are probably as follows: $^2J(Sn-H_{cis})$, $^2J(Sn-P_{cis})$, and $^1J(Rh-Sn)$ positive; $^1J(Rh-H)$, $^1J(Rh-P)$, and $^2J(P-H_{cis})$ negative. [6] [g] $J(^{119}Sn-^1H) \sim J(^{117}Sn-^1H)$. [h] $J(^{119}Sn-^{31}P)$ was measured from the ^{119}Sn spectrum. [i] For **1a** in $CDCl_3$ $\delta(P) = 42.42$, $\delta(Rh) = 333$ ppm; in toluene $\delta(P) = 42.89$, $\delta(Rh) = 336$ ppm (300 K). [j] Prepared in situ. [k] Values in parentheses were obtained at 213 K. [l] Signal broadened at 213 K.

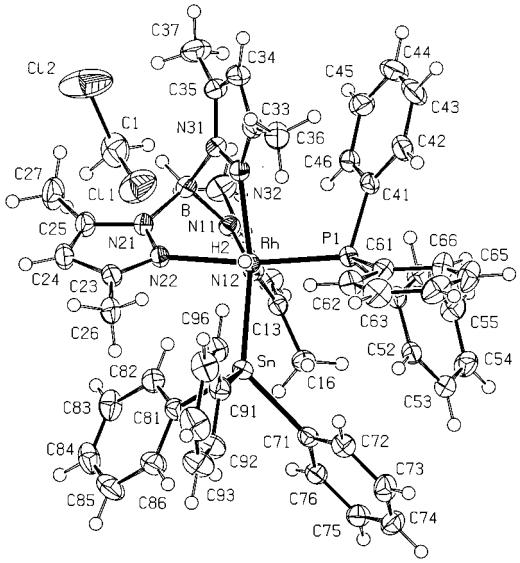

Figure 4. ORTEP diagram of $[Rh(Tp^*)(H)(SnPh_3)(PPh_3)](CH_2Cl_2)$ (**4a**). Thermal ellipsoids are shown at the 50% probability level. The hydride ligand was located.

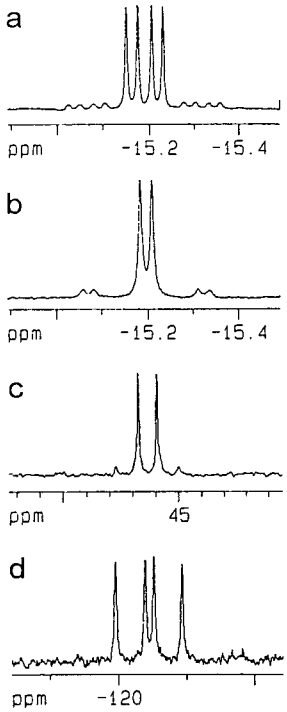

Figure 5. NMR spectra obtained from $[Rh(Tp^*)(H)(SnPh_3)(PPh_3)]$ (**4a**) in dichloromethane at 300 K: (a) ^1H; (b) $^1H\{^{31}P\}$; (c) $^{31}P\{^1H\}$; (d) $^{119}Sn\{^1H\}$.

tion of PPh_3 (0.4 M) to a solution of **1a** (0.006 M) causes no significant change in the low-temperature $^{31}P\{^1H\}$ spectrum, indicating that phosphine dissociation is unlikely to contribute to the broadening of the ^{31}P signal. The reluctance of **1a,b** to bind Tp* in a tridentate manner can be attributed to the presence of a fairly high electron density on the metal (pyrazole is a good σ-donor but a poor π-acceptor). Complexes **2**−**4**, with η^3-Tp*, have rhodium in oxidation state +3.

For each of complexes **2**−**4** the signal from the hydride ligand appears at low δ (∼−15 ppm) and shows spin coupling of ^1H to ^{31}P and ^{103}Rh (Figure 5a,b). In the case of **4** satellite signals are observed indicating coupling to ^{117}Sn and ^{119}Sn (which have natural abundance 7.6% and 8.6%, respectively). The coupling of the two isotopes to ^1H cannot be distinguished as the values of $J(^{117}Sn-^1H)$ and $J(^{119}Sn-^1H)$ are very similar. Satellite peaks are also observed associated with the ^{31}P signal (Figure 5c). The ^{119}Sn signal is shown in Figure 5d.

In a recently reported study of several complexes $[Rh(X)(H)(SnPh_3)(PPh_3)(L)]$ (X = e.g. $NCBPh_3$, $N(CN)_2$; L = pyridine and substituted pyridines)[6] clear trends were found in both $\delta(^{119}Sn)$ and $J(Sn-H)$ that related to the electron-donating properties of ligands. Data for **4a,b** (recorded at 213 K so as to be comparable to data in ref 6) fit this pattern quite closely. While good evidence exists for the presence of three-center Rh−H−Sn bonds in the complexes on which the earlier study is based, the same cannot be said of complex **4a** (and, by implication, **4b**) for which the Sn−H distance indicates bonding that is much closer to a full oxidative addition product.

The purpose of varying the phosphine in complexes **1**−**4** is to discover any differences in properties that might arise from a small change in the electron density on rhodium (for **1**−**3** yields of the fluorophosphine complexes, **b**, are slightly lower than those of the corresponding PPh_3 complexes, **a**; in the case of **3b** a pure product cannot be isolated) and to determine the influence on NMR parameters of such changes. No significant difference is observed in $\delta(^1H)$ on replacing

PPh_3 by $P(C_6H_4F)_3$ in **2** and **4**. In $^{31}P\{^1H\}$ spectra, however, signals from the fluorophosphine complexes are shifted to lower δ by ~2 ppm; in ^{103}Rh spectra the shift is 3−19 ppm, and in ^{119}Sn spectra it is ~5 ppm relative to the triphenylphosphine complex. These values do not differ greatly from those measured for the complexes $[Rh(Cl)(H)(SnPh_3)(PR_3)(py)]$ (R = Ph, C_6H_4F),[6] which show shifts to lower δ of 1.76 ppm (^{31}P), 16 ppm (^{103}Rh), and 5.5 ppm (^{119}Sn) on exchanging PPh_3 for $P(C_6H_4F)_3$.[6] The effects on coupling constants other than J(Sn−H) and J(Rh−Sn) are marginal. Both J(Sn−H) and J(Rh−Sn) decrease slightly on going from **4a** to **4b**, in keeping with the trend observed for complexes $[Rh(Cl)(H)(SnPh_3)(PR_3)(py)]$.

The ^{103}Rh chemical shift differences of ~300 ppm between **2a,b** and **3a,b** (rhodium bonded to carbon in each case) can be attributed to local magnetic fields generated by π electrons in the acetylide and carbonyl groups; in **2a,b** the field experienced at Rh is shielding, and in **3a,b** it is deshielding. The rhodium chemical shift is also influenced by the hard/soft properties of ligands,[26] the presence of a soft ligand (e.g. $SnPh_3$) being associated with a shift to low δ (as observed).

Acyl Complex. In toluene at 70 °C **3a** (0.01 M) decomposes to the extent of 30% after 21 h (i.e. 70% is unchanged) as determined from ^{31}P NMR spectra. For an acyl hydride complex this is evidence of unusually high thermal stability. The decomposition product, which was not isolated, was identified as [Rh(Tp*)(PPh$_3$)(CO)] by comparison of ^{31}P data {toluene, 300 K δ(^{31}P) 43.27, d, J($^{103}Rh-^{31}P$) 161.3 Hz} with data reported by Connelly and co-workers.[13] The extent of decomposition is not significantly affected by the addition of triphenylphosphine (0.15 M), indicating that Tp* chelate ring opening rather than phosphine dissociation is responsible for the creation of a vacant coordination site (see below).

The majority of acyl hydride complexes that have been structurally characterized are stabilized by chelating or (where more than one metal atom is involved) bridging interactions, while others exhibit features such as η^2 or η^3 binding of the acyl CO which are also likely to be stabilizing. Exceptions are $[Rh\{N(CH_2CH_2PPh_2)_3\}(H)(COMe)](BPh_4)$[23] $[Rh(COPh)(H)(Cl)(P^iPr_3)_2]$,[24] $[Ir(COCH_2OH)(H)(Cl)(PMe_3)_3]$,[27] $[Pt(4,4'\text{-}^tBu_2bipy)(COMe)_2(H)(Cl)]$,[28] and $[Ir(Cp^*)(CO^tBu)(H)(PMe_3)]$[29] (in addition to **3a**), which have unsupported acyl and hydride ligands, with evidence of H···H contacts in the case of $[Rh(COPh)(H)(Cl)(P^iPr_3)_2]$[24] and of **3a** and an O···H hydrogen bond in the case of $[Ir(COCH_2OH)(H)(Cl)(PMe_3)_3]$.[27] In the absence of stabilizing bonds an acyl hydride complex might normally be expected (upon generation of a vacant coordination site) to undergo extrusion of CO (from COR) followed by the irreversible reductive elimination of RH (the basis of the catalyzed decarbonylation of aldehydes[30]). This is indeed found for $[Rh(COPh)(H)(Cl)(P^iPr_3)_2]$,[24] in which a vacant site already exists. The complex decomposes rapidly in solution at ambient temperatures (to give C_6H_6 and $[Rh(Cl)(CO)(P^iPr_3)_2]$), the decomposition being greatly inhibited by an excess of P^iPr_3.[24]. Other complexes noted above all have high thermal stability: this is attributed, for $[Ir(COCH_2OH)(H)(Cl)(PMe_3)_3]$, to tight binding of the phosphines.[27] The presence of multidentate ligands (such as Tp* in **3a**) should further reduce the likelihood that decomposition will occur via the formation of a vacant site.

Acknowledgment. We thank the University of the Witwatersrand for financial support.

Supporting Information Available: Crystallographic tables in CIF format for compounds **1a**, **2b**, **3a**, and **4a**. This material is available free of charge via the Internet at http://pubs.acs.org.

IC0112037

(26) Mann, B. E. In *Transition Metal NMR*; Pregosin, P. S., Ed.; Elsevier: Amsterdam, 1991; pp 177−215.

(27) Milstein, D.; Fultz, W. C.; Calabrese, J. C. *J. Am. Chem.* Soc. **1986**, *108*, 1336.

(28) (a) Gerisch, M.; Bruhn, C.; Vyater, A.; Davies, J. A.; Steinborn, D. *Organometallics* **1998**, *17*, 3101. (b) Steinborn, D.; Vyater, A.; Bruhn, C.; Gerisch, M.; Schmidt, H. *J. Organomet. Chem.* **2000**, *597*, 10.

(29) Peterson, T. H.; Golden, J. T.; Bergman, R. G. *Organometallics* **1999**, *18*, 2005.

(30) Baird, M. C.; Nyman, C. J.; Wilkinson, G. *J. Chem. Soc. A* **1968**, 348.